PHYSICAL REVIEW APPLIED 8, 061001 (2017)

Shaping Microwave Fields Using Nonlinear Unsolicited Feedback: Application to Enhance Energy Harvesting

Philipp del Hougne, Mathias Fink, and Geoffroy Lerosey

Institut Langevin, CNRS UMR 7587, ESPCI Paris, PSL Research University, 1 rue Jussieu, 75005 Paris, France

(Received 5 June 2017; revised manuscript received 12 September 2017; published 27 December 2017)

Wave-front shaping has emerged over the past decade as a powerful tool to control wave propagation through complex media, initially in optics and more recently also in the microwave domain with important applications in telecommunication, imaging, and energy transfer. The crux of implementing wave-front shaping concepts in real life is often its need for (direct) feedback, requiring access to the target to focus on. Here, we present the shaping of a microwave field based on indirect, unsolicited, and blind feedback which may be the pivotal step towards practical implementations. With the example of a radio-frequency harvester in a metallic cavity, we demonstrate tenfold enhancement of the harvested power by wave-front shaping based on nonlinear signals detected at an arbitrary position away from the harvesting device.

DOI: 10.1103/PhysRevApplied.8.061001

As a wave propagates through a complex medium, its initial wave front is completely scrambled due to multiple scattering and reflection events occurring inside the medium [1]. Depending on the wave type, very different environments may be considered complex; a thin layer of paint, biological tissue, or a multimode fiber at optical wavelengths and cities or disordered cavities for microwaves are common examples [1–6]. Formerly, this complete scrambling was perceived as absolutely detrimental to information transfer which in turn is crucial for imaging and communication applications. More recently, various novel techniques emerged that embrace the secondary sources offered by complex media rather than considering them an obstacle. Around the turn of the millennium, the information capacity achievable with MIMO communication systems in complex media was shown to outperform that of free space [6,7], and time reversal was developed in acoustics and then also for microwaves [8,9]. A bit later, wave-front shaping was introduced in optics [10].

Since then, wave-front shaping in complex media has enabled fascinating demonstrations such as focusing beyond the Rayleigh limit [11–14], the spatiotemporal refocusing of distorted pulses [15–17], and subsampled compressive imaging [18], to name a few. Furthermore, measuring the complex medium's transmission matrix [19–24] provided information about important statistical properties and the transmission eigenchannels of the medium [25–27], as well as being an open-loop tool in contrast to iterative focusing algorithms.

However, ten years after Vellekoop and Mosk's first demonstration in optics [10], focusing by wave-front shaping has not yet become an omnipresent technique in commercial imaging devices, medical therapy, or the telecommunication industry. A challenging hurdle on the path from academic proof of concepts towards real-life applications is usually the need for a feedback signal from the target point(s) to focus on, a common characteristic of all wave-front shaping techniques. For medical applications, a camera cannot be placed inside the biological tissue and implanting objects that generate fluorescence or harmonics might be too invasive. Similarly, improving signal reception on a wireless device in an indoor environment by wave-front shaping [28] requires real-time access to the device's received signal strength indicator, which is possible to some extent in Wi-Fi, for instance, but difficult to imagine for low-energy Internet of Things (IOT) devices.

These difficulties with direct feedback motivate the identification of indirect feedback schemes. Indirect solicited feedback about the target intensity was already successfully employed in fluorescence experiments in optics [29]; indirect unsolicited feedback has been demonstrated with magnetic-resonance-guided ultrasound focusing in acoustics and by exploiting either the photoacoustic effect or two-photon fluorescence in optics, all using biological tissue [30–32]. In this Letter, we transpose this concept of wave-front shaping with indirect unsolicited feedback to the microwave domain. Our target to focus on is a nonlinear device, a radio-frequency (rf) harvester, that captures the ambient microwave signal and rectifies it into a dc output. The rectification involving diodes is a nonlinear process inevitably generating nonlinear signals that are reemitted and constitute our indirect feedback.

Incidentally, our work addresses a key challenge of current rf harvesting setups: the harvested voltages are too low for real-life applications [33]. Potentially, rf harvesting is a promising technique in the advent of concepts such as Smart Home and the Internet of Things. It may enable the wireless and battery-free powering of many low-power sensors, recycling the energy of the ubiquitous rf fields in

our urban environments and thereby constituting a step towards a greener future.

Using simple electronically reconfigurable reflector arrays, so-called spatial microwave modulators (SMMs) [34], we create constructive interferences of the reflected waves at the position of the harvester. Thereby, we focus the wave field and enhance the harvested energy that depends in a monotonic but nonlinear way on the incident field intensity. First, we demonstrate in the controlled environment of a disordered microwave cavity the significant enhancement of the harvester's voltage output by optimizing the incident wave front, using the harvested voltage as direct feedback. Second, we maximize once again the harvested voltage, but this time using an indirect unsolicited feedback: the strength of nonlinear signatures detected inside the cavity at an arbitrary location away from the harvester.

We use a disordered metallic cavity (1.1 m^3; $Q = 835$) that constitutes a static, well-controllable complex medium for our proof-of-concept experiments. In the microwave domain, reverberant media are very common: electromagnetic compatibility tests require reverberation chambers [35–37], open disordered cavities currently attract a lot of interest for computational imaging [38–41], and indoor environments trap telecommunication signals [6,28]. The SMM covers roughly 7% of the cavity walls with 102 binary elements whose boundary conditions can be switched dynamically between Dirichlet and Neumann for frequencies within a 100-MHz bandwidth around 2.47 GHz; their working principle is outlined in the inset in Fig. 1 and in Ref. [34].

With an arbitrary signal generator (sampling at 10 GHz), we mimic a continuously excited ambient field by emitting a 30-μs-long signal within the 2.4-GHz Wi-Fi band; a bandpass filter (2.38–2.52 GHz) cleans the signal before it is emitted into the cavity by a monopole antenna adapted for Wi-Fi frequencies in free space.

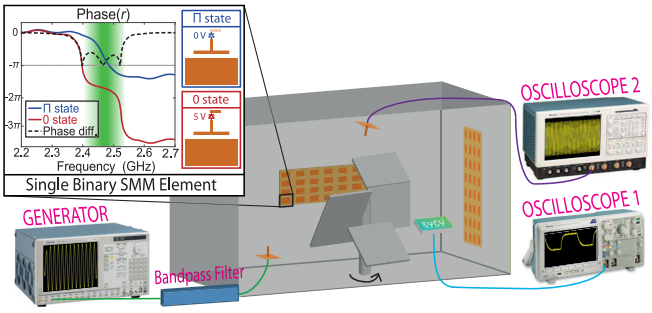

FIG. 1. Schematic of experimental setup. Using a wave generator, a quasicontinuous ambient field is generated inside a disordered metallic cavity. This field can be shaped with spatial microwave modulators that partially cover the cavity walls. Oscilloscope 1 monitors the voltage output of a radio-frequency harvester. The high-sampling-rate oscilloscope 2 is used to analyze the spectrum at an arbitrary position away from the harvester. A mode-stirrer rotation by 12° conveniently realizes disorder. The inset is adapted from Ref. [34].

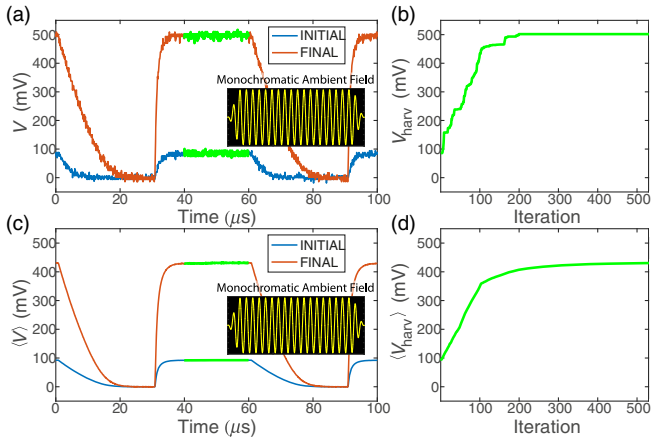

FIG. 2. Experimental method exemplified for a monochromatic ambient field using direct feedback. (a) shows the harvester's voltage output, monitored on oscilloscope 1, before (blue) and after (red) optimization. The interval chosen to estimate V_{harv} is indicated in green, and the evolution of V_{harv} over the course of the iterative optimization is displayed in (b). (c) and (d) show the quantities presented in (a) and (b) averaged over 300 realizations of disorder.

The rf harvester is a commercial prototype (cf. acknowledgments) that uses a low-power Schottky diode circuit to rectify the captured microwave signal [42]. The results we present stand on their own and are independent of the harvester's detailed operating mode. The employed device harvests most efficiently around 2.42 GHz. With the low-frequency oscilloscope 1 (1 MΩ; 100 MHz; 8 bits), triggered by the generator, we monitor the harvested voltage. As exemplified in Fig. 2(a), it takes a few microseconds for the harvested voltage to rise, and a bit longer to decay after the excitation signal stops. The repetition rate of the generator is chosen such that the cycles do not overlap; over a 20-μs interval [highlighted in green in Fig. 2(a)], the harvested signal is stationary. In the following, harvested voltage V_{harv} refers to the average signal received during this stable interval.

For the indirect feedback scheme in the second part, a further Wi-Fi monopole antenna is placed at an arbitrary location inside the cavity outside the harvester's line of sight; the high-sampling-rate oscilloscope 2 measures the received signal, again triggered by the generator. A 2-μs interval, sampled at 25 GHz and averaged over 50 measurements, is acquired and then Fourier transformed to quantify the intensity of nonlinear signals in the spectrum. Using adapted antennas, appropriate filters, or lock-in detection would be simple, cheap, and well-established means to improve the acquisition robustness and simultaneously remove the need for the costly oscilloscope 2. Note that the frequency of optimal operation varies across our employed equipment (monopole antennas, SMM, harvester); while this does not hinder the intended proof of concept, quantitatively even better results are to be expected with refined equipment.

Work with disordered media usually requires averaging over many realizations of disorder to get a representative idea of the underlying physics. An individual optimization outcome strongly depends on the initial conditions, e.g., whether the specklelike field initially has a node or antinode at the target position. We conveniently realize disorder with the mode stirrer indicated in Fig. 1: rotating it by 12° yields a "new" disordered cavity with the same global parameters (volume, quality factor, etc.) but a different geometry, enabling a total of 30 independent realizations. As the SMM has a large control over the wave field in this setup [43], the experiment can, moreover, be repeated several times for each mode-stirrer position, starting with a different random SMM configuration each time. Random SMM configurations effectively constitute different cavity geometries preserving the global parameters, too.

To begin with, we consider the case of an ambient monochromatic field that we would like to harvest, using the harvested voltage as direct feedback. To identify the optimum SMM configuration, we use an iterative continuous sequential optimization algorithm [44]. Element after element, it tests which of the two possible SMM states brings us closer to our objective of maximizing a chosen cost function (CF), here $\mathrm{CF} = V_{\mathrm{harv}}$. This procedure is summarized in Fig. 2, where we show the harvester output before and after optimization in (a) and the dynamics of the optimization in (b); (c) and (d) present the same quantities averaged over 300 realizations of disorder. Note that the number of iterations required until saturation in (b) is about twice the number of SMM pixels. Unlike the first optics experiments that used this iterative method to focus through multiply scattering paint layers, we cannot limit ourselves to testing each element only once; instead we have to retest them several times due to the reverberation that correlates the optimum states of different elements.

Next, we explore how the harvesting enhancement by wave-front shaping with our setup depends on the ambient monochromatic field's frequency and power. The generator's peak-to-peak voltage V_{PP} is used to alter the ambient field's power. Each resulting data point displayed in Fig. 3(a) is the average over 300 realizations. Here, we chose a representation in terms of voltage (rather than power), as the minimum voltage requirements, even by dc-dc converters, were identified as a key limiting factor in Ref. [33] for harvesting schemes to be useful in practice. Since our employed equipment's frequency responses are not flat, a slight frequency dependence is evident in Fig. 3(a). The power dependence may be surprising, since power is not a variable appearing in the theoretical model used to explain traditional monochromatic wave-front shaping experiments in terms of degrees of freedom [43]. This can be understood, however, from the fact that V_{harv} depends in a monotonic but not necessarily linear manner on the ambient monochromatic field's intensity $|S(f_0, \mathbf{r}_0)|^2$ at the harvester's position $\mathbf{r}_0$. Here, the mean voltage enhancements vary between about 4 and 6, the corresponding power enhancements thus

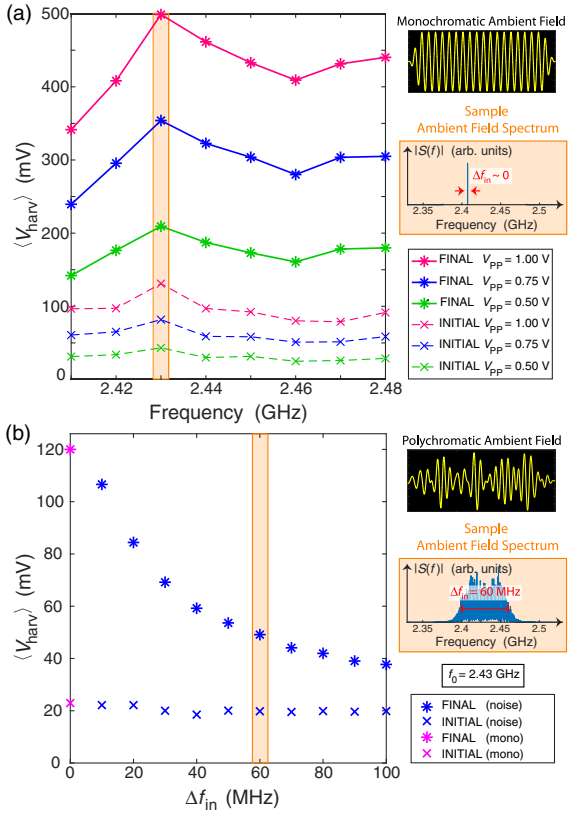

FIG. 3. The harvested voltages before and after direct feedback based wave-front shaping, (a) for monochromatic fields of different frequencies and powers (cf. legend), averaged over 300 realizations of disorder; (b) for polychromatic (noise) fields of different bandwidths Δf_{in}, centered on $f_0 = 2.43$ GHz, averaged over 150 realizations.

being on the order of 20 to 30; the attained enhancement is larger for weaker ambient fields. This power dependence, likely to be generalizable to most harvesting devices, works in favor of our proposal to enhance harvesting by wave-front shaping, in particular in the case of (realistic) weak ambient fields.

How well does wave-front-shaping-based harvesting enhancement do in a more realistic, polychromatic ambient field? To explore this question, we work with noise signals [45], emitted by the generator, of different bandwidths Δf_{in} centered on 2.43 GHz. We observe a clear decrease of the achievable voltage enhancement from a factor of about 5 to a factor of about 2, as Δf_{in} is increased. This tendency can be understood with traditional wave-front shaping tools. In the case of a polychromatic ambient field, the harvested voltage is essentially equivalent to incoherent polychromatic focusing with unknown weights $w(f)$ for different frequencies: $V_{\mathrm{harv}} \approx \int_{\Delta f_{\mathrm{in}}} w(f)|S(f)|^2 df$. Wave-front shaping can relocate a certain amount of energy that is on average equally spread across the $1 + \Delta f_{\mathrm{in}}/\Delta f_{\mathrm{corr}}$ independent frequencies, where $\Delta f_{\mathrm{corr}} = f_0/Q$ is the cavity correlation frequency; the literature contains multiple reports confirming this experimentally [46–50]. In Fig. 3(b)

the decrease of the attainable enhancement is quite drastic as our highly reverberating cavity has a correlation frequency of a few MHz, implying a high number of independent frequencies inside Δf_{in}. Yet in lossier and leakier real-life systems Δf_{corr} would be rather on the order of a few tens of MHz such that real scenarios would stay within the very upper part of the curve, not experiencing major drawbacks from broadband operation.

Having demonstrated the viability of wave-front shaping to enhance the harvested voltages both in monochromatic and polychromatic ambient fields using direct feedback, we now turn to the indirect feedback case. The diode-based rectifier circuit inside the harvester is intrinsically a source of nonlinearities that are reemitted into the cavity by the harvester's receiving antenna. Approximated to first order, the strength of the nonlinear reemissions increases monotonically as the excitation intensity incident on the harvester $|S(f_0, \mathbf{r}_0)|^2$ rises. The intensity $|S(f_{\text{NL}}, \mathbf{r}_{\text{NL}})|^2$ of a nonlinear signature of frequency f_{NL} at position $\mathbf{r}_{\text{NL}}$ away from the harvester may thus serve as feedback about the excitation intensity incident on the harvester that is unsolicited as it is generated naturally and inevitably. Moreover, it constitutes a blind feedback in the sense that we focus the wave field on the harvester without any knowledge of its position $\mathbf{r}_0$ in space.

Under which circumstances will $\text{CF} = |S(f_{\text{NL}}, \mathbf{r}_{\text{NL}})|^2$ provide a reliable feedback about $|S(f_0, \mathbf{r}_0)|^2$? Changes in $|S(f_{\text{NL}}, \mathbf{r}_{\text{NL}})|^2$ must occur *only* in response to changes in $|S(f_0, \mathbf{r}_0)|^2$. If there were sources other than the harvester emitting at f_{NL}, the detected magnitude $|S(f_{\text{NL}}, \mathbf{r}_{\text{NL}})|^2$ of the interference of all those f_{NL} sources would be sensitive to relative phase differences between the sources. Similarly, if the wave field at f_{NL} was modulated by the SMM, the value measured for $|S(f_{\text{NL}}, \mathbf{r}_{\text{NL}})|^2$ would heavily depend on the SMM state, as well as on $|S(f_0, \mathbf{r}_0)|^2$. Fortunately, neither of those scenarios arises in our setup; otherwise, either or both could be circumvented by working with $\langle |S(f_{\text{NL}}, \mathbf{r}_{\text{NL}})|^2 \rangle_{\text{independent } \mathbf{r}_{\text{NL}}}$, the average of $|S(f_{\text{NL}}, \mathbf{r}_{\text{NL}})|^2$ over several independent positions $\mathbf{r}_{\text{NL}}$.

To demonstrate the feasibility of the indirect feedback-based harvesting enhancement scheme, we here choose to work with a monochromatic ambient field at 2.43 GHz and limit ourselves to 90 realizations, as our setup is not optimized in terms of speed. In the top row of Fig. 4 we present the example of $f_{\text{NL}} = 2f_0$, illustrating both a single realization and the average over 90 realizations of disorder. On the left in Fig. 4(a), we show the evolution of the nonlinear feedback signal, over the course of the iterative optimization. On the right in Fig. 4(b), we display how the harvested voltage at the target position is enhanced. Nonlinearities being naturally weak in comparison to the excitation signal, the individual realization suffers notably more from noise than in Fig. 2(b), where we used the harvested voltage as direct feedback.

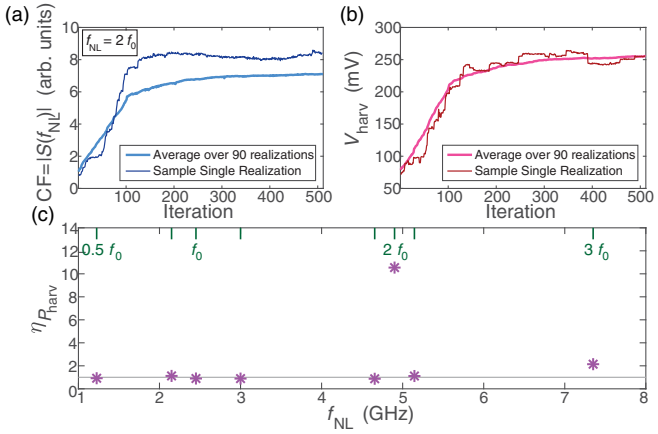

FIG. 4. Wave-front shaping with indirect, unsolicited, blind feedback $\text{CF} = |S(f_{\text{NL}}, \mathbf{r}_{\text{NL}})|^2$. For the monochromatic case with $f_{\text{NL}} = 2f_0$, we display the optimization dynamics of the cost function in (a) and the corresponding harvested voltage in (b), both for a single realization and the average over 90 realizations of disorder. The average enhancement of the harvested power $\eta_{P_{\text{harv}}} = \eta^2_{V_{\text{harv}}}$ is displayed in (c) for a range of different choices of f_{NL}.

The achieved mean enhancement of the harvested voltage of 3.3, albeit being substantial and corresponding to a tenfold enhancement of the harvested power, is, nonetheless, notably lower than the results from direct feedback seen in Fig. 3(a). This can of course be attributed, in particular, to the unfavorable dynamic range of our temporal measurement of $|S(f_{\text{NL}}, \mathbf{r}_{\text{NL}})|^2$.

Furthermore, we test frequencies other than $2f_0$ to provide indirect feedback, the results being on display in Fig. 4(c), in terms of the average enhancement of the harvested power $\eta_{P_{\text{harv}}} = \eta^2_{V_{\text{harv}}} = \langle V^{\text{fin}}_{\text{harv}} \rangle^2 / \langle V^{\text{init}}_{\text{harv}} \rangle^2$. It can be seen that only $2f_0$ and $3f_0$ result in an enhancement of the harvested voltage, which is significantly stronger in the case of $2f_0$. This confirms that, as one might have anticipated intuitively, the best candidate to work with is the second harmonic [51,52]. At $f_{\text{NL}} = f_0$, the quantity $|S(f_0, \mathbf{r}_{\text{NL}})|^2$ has of course been heavily enhanced but this did not correlate at all with the evolution of $|S(f_0, \mathbf{r}_0)|^2$: the value of $|S(f_0, \mathbf{r}_{\text{NL}})|^2$ is dominated by the SMM's state and the emitted excitation signal. The other tested frequencies are arbitrary, thus not corresponding to any nonlinear signatures, such that they do not yield any enhancement either. We also verified that results similar to the ones presented in Fig. 4 are obtained for different $\mathbf{r}_{\text{NL}}$ and f_0, but they are omitted for clarity's sake here.

To conclude, in this Letter we started off by proving that shaping an ambient microwave field in a reverberant medium to concentrate it on a radio-frequency harvester may constitute an innovative improvement to current rf harvesting schemes that typically do not harvest sufficiently high voltages. Using the harvested voltage as direct feedback, we demonstrated significant harvesting enhancements

both for a variety of monochromatic and polychromatic wave fields. Then, we exploited the nonlinear nature of the diode-based harvesting device that inevitably causes the reemission of nonlinear signatures into the cavity. By measuring the intensity of the second harmonic at an arbitrary position away from the harvester, we obtained an indirect, unsolicited, and blind feedback about the ambient field intensity at the harvester. This enabled a tenfold enhancement of the harvested power with our current setup.

Using indirect, unsolicited, and blind feedback, removing the need to access the target or its spatial position directly, may be the crucial bridge between an academic concept of focusing by wave-front shaping and its application in practice, in many cases. We expect our work to be particularly useful for emerging concepts such as Smart Homes that envisage to populate homes and factories with many low-power sensors. With the aid of spatial microwave modulators (SMMs), IOT devices and sensors could be powered wirelessly, harvesting the ambient omnipresent rf fields. Improving the SMM design [34,53–55], matching the operating bandwidths of SMM and harvester, as well as covering more than only 7% of the walls with SMMs should easily enable much higher enhancements than reported here and counterbalance the decrease in wave-front shaping ability of the SMM in less reverberant (lower Q) realistic environments [43]. Using nonlinear feedback is expected to simultaneously compress the impulse response of *pulsed* ambient fields temporally [16,56], but realistic communication signals typically have time-bandwidth products orders of magnitude above unity [33]. Multitarget focusing [10,24] may require additional techniques like frequency tagging to avoid focusing only on the target emitting the strongest nonlinearity [32]. For other applications such as wireless phone charging that require a lot more power than available in the ambient rf fields, an active emission is certainly necessary; employing our indirect feedback approach might be considered in such wireless power transfer [57–59] scenarios, too.

We gratefully acknowledge the start-up SYCY [60] for providing us with a prototype of their rf harvester. P. d. H. acknowledges funding from the French "Ministère de la Défense, Direction Générale de l'Armement." This work is supported by LABEX Wi-Fi (Laboratory of Excellence within the French Program "Investments for the Future") under Grants No. ANR-10-LABX-24 and No. ANR-10-IDEX-0001-02 PSL.

[1] A. P. Mosk, A. Lagendijk, G. Lerosey, and M. Fink, Controlling waves in space and time for imaging and focusing in complex media, Nat. Photonics **6**, 283 (2012).

[2] M. Kim, W. Choi, Y. Choi, C. Yoon, and W. Choi, Transmission matrix of a scattering medium and its applications in biophotonics, Opt. Express **23**, 12648 (2015).

[3] T. Čižmár and K. Dholakia, Shaping the light transmission through a multimode optical fibre: Complex transformation analysis and applications in biophotonics, Opt. Express **19**, 18871 (2011).

[4] Y. Choi, C. Yoon, M. Kim, T. D. Yang, C. Fang-Yen, R. R. Dasari, K. J. Lee, and W. Choi, Scanner-Free and Wide-Field Endoscopic Imaging by Using a Single Multimode Optical Fiber, Phys. Rev. Lett. **109**, 203901 (2012).

[5] W. Xiong, P. Ambichl, Y. Bromberg, B. Redding, S. Rotter, and H. Cao, Principal modes in multimode fibers: Exploring the crossover from weak to strong mode coupling, Opt. Express **25**, 2709 (2017).

[6] S. H. Simon, A. L. Moustakas, M. Stoytchev, and H. Safar, Communication in a disordered world, Phys. Today **54**, No. 9, 38 (2001).

[7] A. L. Moustakas, H. U. Baranger, L. Balents, A. M. Sengupta, and S. H. Simon, Communication through a diffusive medium: Coherence and capacity, Science **287**, 287 (2000).

[8] M. Fink, Time reversed acoustics, Phys. Today **50**, No. 3, 34 (1997).

[9] G. Lerosey, J. de Rosny, A. Tourin, A. Derode, G. Montaldo, and M. Fink, Time Reversal of Electromagnetic Waves, Phys. Rev. Lett. **92**, 193904 (2004).

[10] I. M. Vellekoop and A. P. Mosk, Focusing coherent light through opaque strongly scattering media, Opt. Lett. **32**, 2309 (2007).

[11] Y. Choi, T. D. Yang, C. Fang-Yen, P. Kang, K. J. Lee, R. R. Dasari, M. S. Feld, and W. Choi, Overcoming the Diffraction Limit Using Multiple Light Scattering in a Highly Disordered Medium, Phys. Rev. Lett. **107**, 023902 (2011).

[12] E. G. van Putten, D. Akbulut, J. Bertolotti, W. L. Vos, A. Lagendijk, and A. P. Mosk, Scattering Lens Resolves Sub-100 nm Structures with Visible Light, Phys. Rev. Lett. **106**, 193905 (2011).

[13] J.-H. Park, C. Park, H. Yu, J. Park, S. Han, J. Shin, S. H. Ko, K. T. Nam, Y.-H. Cho, and Y. Park, Subwavelength light focusing using random nanoparticles, Nat. Photonics **7**, 454 (2013).

[14] I. M. Vellekoop, A. Lagendijk, and A. P. Mosk, Exploiting disorder for perfect focusing, Nat. Photonics **4**, 320 (2010).

[15] J. Aulbach, B. Gjonaj, P. M. Johnson, A. P. Mosk, and A. Lagendijk, Control of Light Transmission through Opaque Scattering Media in Space and Time, Phys. Rev. Lett. **106**, 103901 (2011).

[16] O. Katz, E. Small, Y. Bromberg, and Y. Silberberg, Focusing and compression of ultrashort pulses through scattering media, Nat. Photonics **5**, 372 (2011).

[17] P. del Hougne, F. Lemoult, M. Fink, and G. Lerosey, Spatiotemporal Wave Front Shaping in a Microwave Cavity, Phys. Rev. Lett. **117**, 134302 (2016).

[18] A. Liutkus, D. Martina, S. Popoff, G. Chardon, O. Katz, G. Lerosey, S. Gigan, L. Daudet, and I. Carron, Imaging with nature: Compressive imaging using a multiply scattering medium, Sci. Rep. **4**, 5552 (2014).

[19] S. M. Popoff, G. Lerosey, R. Carminati, M. Fink, A. C. Boccara, and S. Gigan, Measuring the Transmission Matrix in Optics: An Approach to the Study and Control of Light Propagation in Disordered Media, Phys. Rev. Lett. **104**, 100601 (2010).

[20] S. Popoff, G. Lerosey, M. Fink, A. C. Boccara, and S. Gigan, Image transmission through an opaque material, Nat. Commun. **1**, 81 (2010).

[21] A. Drémeau, A. Liutkus, D. Martina, O. Katz, C. Schülke, F. Krzakala, S. Gigan, and L. Daudet, Reference-less measurement of the transmission matrix of a highly scattering material using a DMD and phase retrieval techniques, Opt. Express **23**, 11898 (2015).

[22] H. Yu, T. R. Hillman, W. Choi, J. O. Lee, M. S. Feld, R. R. Dasari, and Y. Park, Measuring Large Optical Transmission Matrices of Disordered Media, Phys. Rev. Lett. **111**, 153902 (2013).

[23] M. Mounaix, D. Andreoli, H. Defienne, G. Volpe, O. Katz, S. Grésillon, and S. Gigan, Spatiotemporal Coherent Control of Light through a Multiple Scattering Medium with the Multispectral Transmission Matrix, Phys. Rev. Lett. **116**, 253901 (2016).

[24] P. del Hougne, B. Rajaei, L. Daudet, and G. Lerosey, Intensity-only measurement of partially uncontrollable transmission matrix: Demonstration with wave-field shaping in a microwave cavity, Opt. Express **24**, 18631 (2016).

[25] M. Kim, Y. Choi, C. Yoon, W. Choi, J. Kim, Q.-H. Park, and W. Choi, Maximal energy transport through disordered media with the implementation of transmission eigenchannels, Nat. Photonics **6**, 581 (2012).

[26] I. M. Vellekoop and A. P. Mosk, Universal Optimal Transmission of Light through Disordered Materials, Phys. Rev. Lett. **101**, 120601 (2008).

[27] A. Peña, A. Girschik, F. Libisch, S. Rotter, and A. A. Chabanov, The single-channel regime of transport through random media, Nat. Commun. **5**, 3488 (2014).

[28] N. Kaina, M. Dupré, G. Lerosey, and M. Fink, Shaping complex microwave fields in reverberating media with binary tunable metasurfaces, Sci. Rep. **4**, 6693 (2014).

[29] I. M. Vellekoop, E. G. Van Putten, A. Lagendijk, and A. P. Mosk, Demixing light paths inside disordered metamaterials, Opt. Express **16**, 67 (2008).

[30] B. Larrat, M. Pernot, G. Montaldo, M. Fink, and M. Tanter, Mr-guided adaptive focusing of ultrasound, IEEE Trans. Ultrason. Ferroelectr. Freq. Control **57**, 1734 (2010).

[31] T. Chaigne, O. Katz, A. C. Boccara, M. Fink, E. Bossy, and S. Gigan, Controlling light in scattering media invasively using the photoacoustic transmission matrix, Nat. Photonics **8**, 58 (2014).

[32] O. Katz, E. Small, Y. Guan, and Y. Silberberg, Noninvasive nonlinear focusing and imaging through strongly scattering turbid layers, Optica **1**, 170 (2014).

[33] V. Talla, B. Kellogg, B. Ransford, S. Naderiparizi, S. Gollakota, and J. R. Smith, in *Proceedings of the 11th ACM Conference on Emerging Networking Experiments and Technologies* (ACM, New York, 2015), p. 4, https://dl.acm.org/citation.cfm?id=2836089.

[34] N. Kaina, M. Dupré, M. Fink, and G. Lerosey, Hybridized resonances to design tunable binary phase metasurface unit cells, Opt. Express **22**, 18881 (2014).

[35] D. A. Hill, *Electromagnetic Fields in Cavities: Deterministic and Statistical Theories* (John Wiley & Sons, Hoboken, 2009), Vol. 35.

[36] J.-B. Gros, U. Kuhl, O. Legrand, F. Mortessagne, E. Richalot, and D. V. Savin, Experimental Width Shift Distribution: A Test of Nonorthogonality for Local and Global Perturbations, Phys. Rev. Lett. **113**, 224101 (2014).

[37] J.-B. Gros, U. Kuhl, O. Legrand, and F. Mortessagne, Lossy chaotic electromagnetic reverberation chambers: Universal statistical behavior of the vectorial field, Phys. Rev. E **93**, 032108 (2016).

[38] T. Fromenteze, O. Yurduseven, M. F. Imani, J. Gollub, C. Decroze, D. Carsenat, and D. R. Smith, Computational imaging using a mode-mixing cavity at microwave frequencies, Appl. Phys. Lett. **106**, 194104 (2015).

[39] T. Sleasman, M. F. Imani, J. N. Gollub, and D. R. Smith, Microwave Imaging Using a Disordered Cavity with a Dynamically Tunable Impedance Surface, Phys. Rev. Applied **6**, 054019 (2016).

[40] M. F. Imani, T. Sleasman, J. N. Gollub, and D. R. Smith, Analytical modeling of printed metasurface cavities for computational imaging, J. Appl. Phys. **120**, 144903 (2016).

[41] J. N. Gollub, O. Yurduseven, K. P. Trofatter, D. Arnitz, M. F. Imani, T. Sleasman, M. Boyarsky, A. Rose, A. Pedross-Engel, H. Odabasi *et al.*, Large metasurface aperture for millimeter wave computational imaging at the human-scale, Sci. Rep. **7** (2017).

[42] W. Haboubi, H. Takhedmit, J.-D. Lan Sun Luk, S.-E. Adami, B. Allard, F. Costa, C. Vollaire, O. Picon, and L. Cirio, An efficient dual-circularly polarized rectenna for rf energy harvesting in the 2.45 GHz ISM band, Prog. Electromagn. Res. **148**, 31 (2014).

[43] M. Dupré, P. del Hougne, M. Fink, F. Lemoult, and G. Lerosey, Wave-Field Shaping in Cavities: Waves Trapped in a Box with Controllable Boundaries, Phys. Rev. Lett. **115**, 017701 (2015).

[44] I. M. Vellekoop and A. P. Mosk, Phase control algorithms for focusing light through turbid media, Opt. Commun. **281**, 3071 (2008).

[45] Bandpass filtered long series of numbers generated with MatLab's uniform random number generator.

[46] H. P. Paudel, C. Stockbridge, J. Mertz, and T. Bifano, Focusing polychromatic light through strongly scattering media, Opt. Express **21**, 17299 (2013).

[47] D. Andreoli, G. Volpe, S. Popoff, O. Katz, S. Grésillon, and S. Gigan, Deterministic control of broadband light through a multiply scattering medium via the multispectral transmission matrix, Sci. Rep. **5**, 10347 (2015).

[48] E. Small, O. Katz, Y. Guan, and Y. Silberberg, Spectral control of broadband light through random media by wavefront shaping, Opt. Lett. **37**, 3429 (2012).

[49] F. Van Beijnum, E. G. Van Putten, A. Lagendijk, and A. P. Mosk, Frequency bandwidth of light focused through turbid media, Opt. Lett. **36**, 373 (2011).

[50] C. W. Hsu, A. Goetschy, Y. Bromberg, A. D. Stone, and H. Cao, Broadband Coherent Enhancement of Transmission and Absorption in Disordered Media, Phys. Rev. Lett. **115**, 223901 (2015).

[51] M. Frazier, B. Taddese, B. Xiao, T. Antonsen, E. Ott, and S. M. Anlage, Nonlinear time reversal of classical waves: Experiment and model, Phys. Rev. E **88**, 062910 (2013).

[52] M. Frazier, B. Taddese, T. Antonsen, and S. M. Anlage, Nonlinear Time Reversal in a Wave Chaotic System, Phys. Rev. Lett. **110**, 063902 (2013).

[53] T. H. Hand and S. A. Cummer, Reconfigurable reflectarray using addressable metamaterials, IEEE Antennas Wireless Propag. Lett. **9**, 70 (2010).

[54] S. V. Hum and J. Perruisseau-Carrier, Reconfigurable reflectarrays and array lenses for dynamic antenna beam control: A review, IEEE Trans. Antennas Propag. **62**, 183 (2014).

[55] H. Yang, X. Cao, F. Yang, J. Gao, S. Xu, M. Li, X. Chen, Y. Zhao, Y. Zheng, and S. Li, A programmable metasurface with dynamic polarization, scattering and focusing control, Sci. Rep. **6**, 35692 (2016).

[56] J. Aulbach, A. Bretagne, M. Fink, M. Tanter, and A. Tourin, Optimal spatiotemporal focusing through complex scattering media, Phys. Rev. E **85**, 016605 (2012).

[57] D. R. Smith, V. R. Gowda, O. Yurduseven, S. Larouche, G. Lipworth, Y. Urzhumov, and M. S. Reynolds, An analysis of beamed wireless power transfer in the fresnel zone using a dynamic, metasurface aperture, J. Appl. Phys. **121**, 014901 (2017).

[58] B. Xiao, T. M. Antonsen, E. Ott, and S. M. Anlage, Focusing waves at arbitrary locations in a ray-chaotic enclosure using time-reversed synthetic sonas, Phys. Rev. E **93**, 052205 (2016).

[59] S. K. Hong, V. M. Mendez, T. Koch, W. S. Wall, and S. M. Anlage, Nonlinear Electromagnetic Time Reversal in an Open Semireverberant System, Phys. Rev. Applied **2**, 044013 (2014).

[60] http://www.sycy.fr.